

## Coherent Soliton Communication Lines

O. V. Yushko<sup>a,b\*</sup>, A. A. Redyuk<sup>a,b</sup>, M. P. Fedoruk<sup>a,b</sup>, and S. K. Turitsyn<sup>a,b,c</sup>

<sup>a</sup> Novosibirsk State University, ul. Pirogova 2, Novosibirsk, 630090 Russia

\*e-mail: olesya.yushko@gmail.com

<sup>b</sup> Institute of Computational Technologies, Siberian Branch, Russian Academy of Sciences,  
pr. Akademika Lavrent'eva 6, Novosibirsk, 630090 Russia

<sup>c</sup> Aston Institute of Photonics Technologies, Birmingham, B4 7ET United Kingdom

Received May 8, 2014

**Abstract**—The data transmission in coherent fiber-optical communication lines using solitons with a variable phase is studied. It is shown that nonlinear coherent structures (solitons) can be applied for effective signal transmission over a long distance using amplitude and optical-phase keying of information. The optimum ratio of the pulse width to the bit slot at which the spectral efficiency (transmitted bits per second and hertz) is maximal is determined. It is shown that soliton fiber-optical communication lines can ensure data transmission at a higher spectral efficiency as compared to traditional communication lines and at a high signal-to-noise ratio.

**DOI:** 10.1134/S1063776114100124

### 1. INTRODUCTION

Nonlinear coherent structures play an important role in physics and demonstrate how linear waves can create stable localized objects via nonlinear interactions. In particular, solitons—particle-like solitary nonlinear waves—exist in various physical systems from hydrodynamics to optics [1–6]. Solitons are used in numerous theoretical models and various practical applications. It is known that the development of the theory of optical pulses in nonlinear dispersive media started from work [7], where the possibility of creating optical solitons in optical fibers was predicted, and they were experimentally observed in [8]. The authors of [9] were the first to demonstrate data transmission along fiber communication lines based on optical solitons. Significant progress in the field of soliton data transmission along optical communication line was achieved in the 1990s (see, e.g., [2, 10, 11]). In this work, we discuss the possibility of application of optical solitons for data transmission in coherent (signal phase is used to encode information) fiber communication lines.

Fiber-optical communication lines (FOCLs) provide reliable and high-quality optical signal transmission at a high speed over a distance of many thousands of kilometers [12, 13]. A constant increase in the volume of transmitted information stimulates continuous modification of existing FOCLs and the development of new methods for the transmission of growing data arrays. Actively developing technologies of digital signal processing in coherent communication lines, the methods of spectral channel multiplexing, the methods of generating pulses of a specific shape, and other methods significantly increased the signal rate in mod-

ern communication lines [14–16]. However, in contrast to a radio channel, a fiber communication channel is fundamentally nonlinear: as the signal power increases, the quality of data transmission decreases because of the influence of nonlinear effects in an optical fiber. This influence impose restrictions on the data transmission rate and distance for the traditional (linear) methods of signal encoding, modulation, and transmission developed for linear communication systems [17–19]. The investigation of various compensation methods or the use of nonlinear effects is one of the most important trends in the field of fiber-optics communication. This field is a very good illustration of the application of nonlinear physics methods for solving important practical problems. In this work, we would like to attract attention of the physical community to this technological problem.

We study the nonlinear dynamics of long sequences (time trains) of soliton pulses in the context of coherent soliton communication lines. Soliton pulses appear as a result of a balance between dispersion spreading and the nonlinear Kerr effect in an optical fiber. Single solitons can move along an optical fiber without changing its shape, in contrast to the linear signals used in traditional modulation and encoding formats. Soliton FOCLs, which use a soliton pulse as an information signal carrier, were a popular subject of inquiry [2–6]. However, they have recently ceased to be the main trend in the development of fiber communication lines because of the appearance of new promising technologies.

One of the technical problems of using a soliton for data transmission appears due to the relation between the pulse width and the pulse peak power. If very short

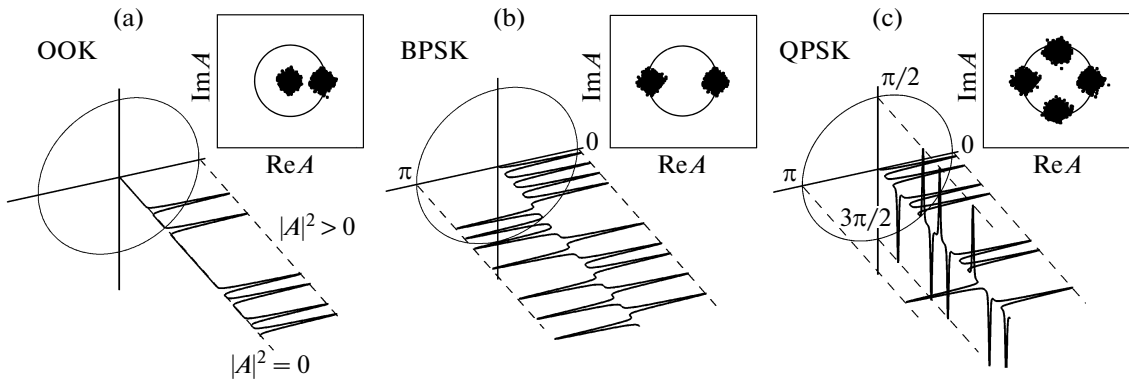


**Fig. 1.** Signal modulation formats: (a) amplitude OOK, (b) binary phase BPSK, and (c) four-level phase QPSK. (insets) Corresponding constellation diagrams (distorted by noise) of a complex signal.

pulses should be used, a too high peak power of solitons is required; this results in significant distortions due to the interaction of such pulses. Although data transmission with solitons was studied in another context, progress in the development of optical coherent communication lines, which use both amplitude (power) and an optical phase for data transmission, makes it possible to apply multilevel modulation formats with a simultaneous decrease in the symbol transmission rate (and the corresponding decrease in the peak soliton power). This specific feature leads to the new opportunities for soliton technologies in data transmission.

In this work, we present the results of a numerical simulation of long-haul transmission links that use coherent methods for data transmission. We found that, for the system parameters and the signal encoding considered here, the spectral efficiency is maximal at a ratio of the bit slot to the soliton width of 1.7 irrespective of the bit rate. It was shown that soliton communication lines can transmit information at a higher signal-to-noise ratio ( $R_{SNR}$ ) as compared to quasi-linear data transmission.

## 2. COHERENT DATA TRANSMISSION

The communication lines of the previous generation use signal amplitude keying: “unit” bit corresponds to a nonzero amplitude pulse, and “zero” bit corresponds to the absence of pulse (on-off-keying (OOK); Fig. 1a). However, coherent data transmission formats, where a pulse phase is used for data keying, are being actively developed.

For example, in the case of the simplest binary phase shift keying (BPSK), “unit” bit corresponds to a pulse with a zero phase and “zero” bit is a pulse of phase  $\pi$  (Fig. 1b). An increase in the number of phase levels used for information encoding allows one pulse to transmit information containing a larger number of bits. For example, two bits can be transmitted by one pulse in the case of quadrature phase shifting keying

(QPSK). For example, sequence 00 can correspond to a zero-phase pulse; 01, to a pulse of phase  $\pi/2$ ; 11, pulse of phase  $\pi$ ; and 10 pulse of phase  $3\pi/2$  (Fig. 1c). When formats of a higher order of keying (such as 8-PSK, 16-PSK, M-PSK) are used, the information rate grows as  $x = \log_2 M$ , where  $M$  is the order of modulation and  $x$  is the number of bits transmitted by one information pulse, due to the fact that one carrying pulse can transmit a larger number of bits.

However, when propagating along an optical fiber, a signal is distorted, and its initial phase changes because of noises and all effects uncompensated at a detector. Such signal distortions are visible in the constellation diagrams shown in the insets to Fig. 1, i.e., diagrams illustrating the phase of each keying pulse at a detector. The larger the distance traveled by a pulse during signal transmission, the larger the distortions. The overlapping of the clouds in the constellation diagrams points to errors upon signal decoding on a quantitative level. The use of keying format with a larger number of phase levels is more effective, since it makes it possible to transmit a larger information bits per symbol. However, this results in faster (when a signal propagates along a line) overlapping of the clouds corresponding to noise and requires additional forces and energy.

The averaged (over periodic amplitude changes because of losses and gain) propagation of optical pulses in fiber communication lines is described by the nonlinear Schrödinger equation (details can be found in, e.g., [2, 3, 5, 11])

$$i \frac{\partial A}{\partial z} - \frac{\beta_2}{2} \frac{\partial^2 A}{\partial t^2} + \gamma |A|^2 A = N(z, t), \quad (1)$$

where  $A$  is the complex envelope of the field,  $z$  is the evolution variable along a line,  $t$  is the time,  $\beta_2$  is the dispersion parameter, and  $\gamma$  is the nonlinearity parameter. Note that the optical losses in communication lines can be continuously compensated using Raman amplification scheme (SRS), so that the average signal power remains constant during its propagation [20,

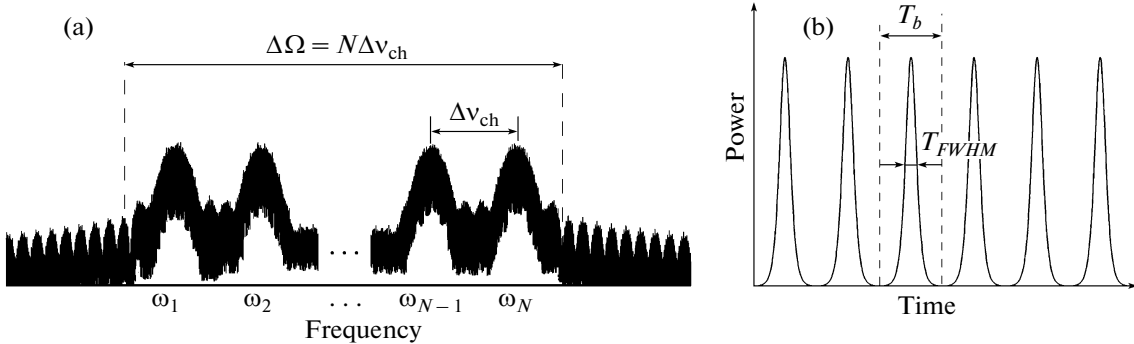


**Fig. 2.** (a) Typical shape of the optical signal spectrum in a multichannel system and (b) typical time distribution of a signal in one channel.

21]. Term  $N(z, t)$  describes noise generation due to amplified spontaneous emission (ASE). As a noise model, we use the model of an additive white Gaussian noise power spectral density per polarization  $N_{ASE} = n_{sp}\hbar\omega\alpha L$ , where  $\omega$  is the frequency,  $\alpha$  is the optical loss factor,  $L$  is the propagation length, and  $n_{sp}$  is the spontaneous emission factor.

It is well known that, in the absence of attenuation and noises at constant dispersion and nonlinearity coefficients, the solution to the Schrödinger equation in the anomalous dispersion range ( $\beta_2 < 0$ ) is the localized soliton pulse

$$A(z, t) = \frac{\sqrt{P_0}}{\cosh(t/T_0)} \exp\left(\frac{iz\gamma P_0}{2}\right), \quad (2)$$

where  $P_0 = |\beta_2|/|\gamma T_0^2|$  is the soliton peak power and  $T_0$  is the time parameter connected to the soliton full width at half-maximum by the relation  $T_{FWHM} \approx 1.763T_0$  (Fig. 2b). The soliton pulse duration determines the signal spectrum width and, correspondingly, spectral data transmission channel width  $\Delta\nu_{ch}$  (Fig. 2a). Apart from the soliton pulse duration, another important parameter that determines the information rate is bit slot  $T_b$  (Fig. 2b). Data transmission rate  $B$  is

$$B = \frac{\log_2 M}{T_b}, \quad (3)$$

where  $M$  is the order of modulation.

To estimate the effect of cumulative noise, parameter  $R_{OSNR} = P_{av}/P_N$ , i.e., the ratio of average signal power  $P_{av}$  to noise power  $P_N$ , is widely used. In soliton FOCLs, the average signal power is defined as

$$P_{av} = \frac{E_s}{T_b} = \frac{2P_0T_0}{T_b}, \quad (4)$$

where  $E_s$  is the soliton pulse energy, and the noise power, e.g., SRS, is determined by the product of noise spectral density  $N_{ASE}$  into characteristic spectral band  $B_{ref}$ . As a rule,  $B_{ref} = 12.5$  GHz is used for engineering

applications. In practice, to estimate the operation of FOCL researchers use the parameter

$$R_{SNR} = \frac{2B_{ref}P_{av}}{R_s P_N}, \quad (5)$$

where  $R_s$  is the symbol rate of data transmission.

Another important characteristic of FOCL is spectral efficiency  $S_{eff}$ , i.e., the ratio of the bit rate of data transmission in one frequency channel to the distance between neighboring frequency channels  $\Delta\nu_{ch}$ ,

$$S_{eff} = \frac{B}{\Delta\nu_{ch}} = \frac{1}{T_b} \frac{\log_2 M}{\Delta\nu_{ch}}. \quad (6)$$

The results of studying the communication lines using traditional (linear) signal modulation methods in terms of the dependence of the spectral efficiency on the signal-to-noise ratio are given in, e.g., [17, 18]. The limitation of spectral efficiency growth was shown to be determined by the nonlinear effects related to the input pulse power. At a high signal-to-noise ratio, a signal is fully distorted and spectral efficiency  $S_{eff} \rightarrow 0$ . Moreover, it was shown that the spectral efficiency is maximal at  $R_{SNR} \approx 20$  dB and that error-free transmission is impossible at  $R_{SNR} > 32$  dB because of nonlinear signal distortions. The main result of nonlinearity is the broadening of a signal spectrum (because of self-phase modulation and cross phase modulation effects) and the appearance of Stokes harmonics in a spectrum. The study of the dependences of the spectral efficiency on  $R_{SNR}$  is of great fundamental interest. Nevertheless, such studies have not yet been performed for soliton FOCLs.

The main property of an optical soliton is the fact that a pulse shape remains unchanged during single soliton propagation along an optical fiber in the absence of noises and optical losses. However, sequences of pulses propagate simultaneously in optical communication lines, which leads to soliton–soliton interaction, namely, mutual attraction or repulsion [1–4]. In spectral multiplexing systems, one has to take into account both intersymbol and interchan-

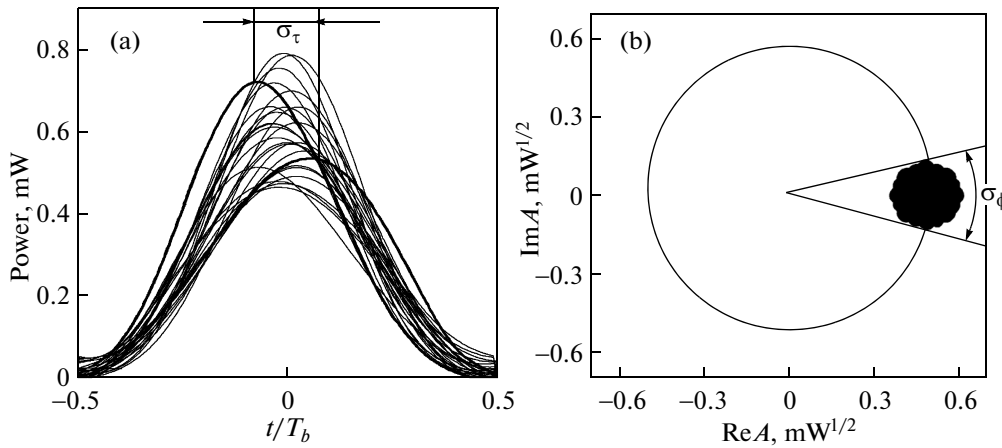


**Fig. 3.** (a) Characteristic picture of timing jitter (many pulses are reduced to one time interval). (b) Determination of phase jitter from a constellation diagram.

nel interaction of pulses from different frequency channels.

Moreover, the interaction of soliton pulses with noise can cause the following undesirable effects: a time shift of a soliton with respect to its initial position and initial soliton phase fluctuations induced by the transformation of amplitude noise into phase noise. These phenomena are known as the Gordon–Haus [3, 22] and Gordon–Mollenauer [3, 23, 24] effects. These effects can be suppressed using distributed signal filtration or the phase conjugation method [3, 25, 26].

Figure 3 schematically shows the quantitative characteristics of timing ( $\sigma_\tau$ ) and phase ( $\sigma_\phi$ ) jitters, which serve as the measure of estimating the soliton pulse parameter fluctuations. The value of  $\sigma_\tau$  is determined by the root-mean-square deviation of a pulse position at a detector from the initial pulse position. In the diagram, all pulses are reduced to one time interval, and this effect manifests itself as the discrepancy between the centers of superimposed pulses. Phase deviations  $\sigma_\phi$  (jitter) are determined as the root-mean-square

Soliton communication line parameters and the signal parameters

Symbol	Value
Dispersion $D$	$17 \text{ ps}^2 \text{ km}^{-1} \text{ nm}^{-1}$
Nonlinearity coefficient $\gamma$	$1.27 \times 10^{-3} \text{ mW}^{-1} \text{ km}^{-1}$
Spontaneous emission parameter $n_{\text{sp}}$	1.0
Signal frequency $\nu$	193.6 THz
Optical loss coefficient $\alpha$	$0.046 \text{ km}^{-1}$
Propagation length $L$	2000 km
Spectral channel width $\Delta\nu_{\text{ch}}$	$2.8 \frac{1.76^2}{\pi^2} \frac{1}{T_{FWHM}} \text{ GHz}$
Number of spectral channels	15

phase deviation and are related to the cloud size in a constellation diagram.

The timing and phase jitters are the main effects that limit the increase of the spectral efficiency with the signal amplitude in soliton FOCLs. For example, an increase in the phase jitter makes it impossible to use high-order modulation formats.

### 3. MATHEMATICAL MODEL

We consider a model soliton FOCL with ideal distributed 2000-km-long Raman amplification scheme [20, 21, 27]. Pulse propagation along an optical fiber is specified by generalized nonlinear Schrödinger equation (1). The parameters are given in the table.

At the receiver, we use the digital backward propagation procedure, which belongs to the methods of digital signal processing. The mathematical implementation of this procedure represents a numerical solution of the nonlinear Schrödinger equation with the opposite sign of a numerical step in evolutional variable  $z$  and in the absence of noise. As the initial condition, we use the signal at the receiving device. This technique is now one of the most promising modern methods for improving the data transmission quality in coherent communication lines, although its real-time application is far from practical implementation [14, 28, 29].

The numerical simulation was based on the split-step Fourier method of second approximation order (see, e.g., [5]). In each calculation, we simulated the propagation of a pseudorandom sequence  $2^{12}$  pulses long in each of the 15 frequency channels. As a phase modulation format, we used a format with a continuous phase distribution and one amplitude level (Fig. 4a). With this modulation format, we can estimate the maximum spectral efficiency [17]. In this work, we propose a simplified method based on the “reverse rotation” of a constellation diagram. After

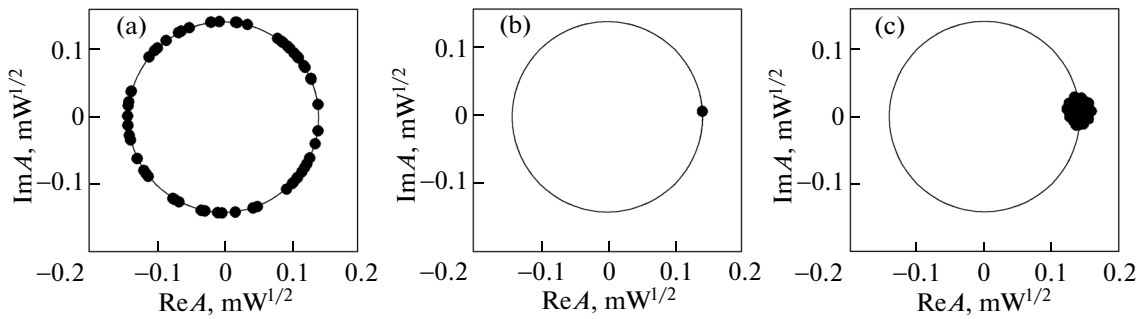


**Fig. 4.** Constellation diagram of a signal: (a) at a receiving device for continuous phase keying, (b) after propagation along a line without noise and the procedure of reverse phase rotation, and (c) after propagation along a line with noise and the reverse phase rotation.

propagation, each point in a constellation diagram is rotated through a certain initial angle specified by deterministic (not related to noise) propagation effects. For example, if the action of noise is weak, the entire constellation diagram transforms into a point after this processing (Fig. 4b). In the reverse case, a certain cloud forms after the rotation of points, and its size is determined by noise or a nonlinear noise–signal interaction (Fig. 4c).

Thus, to estimate the spectral efficiency numerically, we should calculate how many resulting clouds are located at a given amplitude level and then take this number  $M$  as the order of the maximally achieved phase modulation. The spectral efficiency in this case is calculated by the formula

$$S_{\text{eff}} = \frac{B}{\Delta v_{\text{ch}}} = \frac{\log_2 M}{T_b \Delta v_{\text{ch}}} = \frac{\log_2(2\pi\sqrt{P_0}/d)}{T_b \Delta v_{\text{ch}}}, \quad (7)$$

where  $d$  is the cloud diameter.

To analyze the dependence of  $R_{\text{SNR}}$  on bit slot  $T_b$ , we introduce  $T_b/T_{FWHM} = k$ . Substituting the formulas into Eq. (5), we obtain

$$\begin{aligned} R_{\text{SNR}} &= 2 \frac{B_{\text{ref}}}{R_s} R_{OSNR} = 2 \frac{B_{\text{ref}}}{P_N} E_s \\ &= 4 \ln(1 + \sqrt{2}) \frac{2B_{\text{ref}} |\beta_2| k}{P_N \gamma T_b}. \end{aligned} \quad (8)$$

This estimation demonstrates the inverse dependence of parameter  $R_{\text{SNR}}$  on bit slot  $T_b$ : low values of  $R_{\text{SNR}}$  correspond to high values of the bit slot and, hence, low values of symbol rate  $R_s \sim 1/T_b$ . For example,  $R_{\text{SNR}} = 20$  dB (propagation over 2000 km) corresponds to  $T_b = 1.5 \times 10^5$  ps or  $R_s \sim 10^7$  s<sup>-1</sup>. A twofold increase of  $R_{\text{SNR}}$  corresponds to  $T_b \sim 1000$  ps and a data transmission rate of 10<sup>9</sup> s<sup>-1</sup>. At first glance, Eq. (8) makes it possible to conclude that, as the signal-to-noise ratio increases, symbol rate  $R_s$  of data transmission along soliton communication lines increases. This would lead to an increase in the amount of transmitted information and/or the data transmission distance at the same signal quality. However, of course Eq. (8) does not take into account the negative effect

of an increase in the soliton–soliton interaction with the signal peak power and the corresponding degradation of data transmission quality. A quantitative investigation of the balance between various competing effects requires a numerical analysis.

#### 4. RESULTS AND DISCUSSION

Figure 5 shows the results of a numerical simulation of spectral efficiency  $S_{\text{eff}}$  as a function of  $T_{FWHM}$  for various bit slots  $T_b$ . For each curve, the soliton pulse width was varied to reach various values of  $R_{\text{SNR}}$  at a fixed bit slot.

For example, a decrease of  $T_{FWHM}$  leads to an increase in the peak power of a soliton pulse and, hence, an increase in  $R_{\text{SNR}}$ . The spectral channel width (i.e., spectral distance  $\Delta v_{\text{ch}}$  between channels) for each calculation was 2.8 of the soliton spectrum width (full width at half-maximum). This value was chosen for the results of solving the problem of finding the optimum value of  $\Delta v_{\text{ch}}$ . The spectral efficiency decreases to the left of the maximum in each curve because of an increase in the soliton–soliton interaction, and it decreases to the right of the maximum due to the overlapping of broad pulses at a fixed bit slot. We give the values of  $R_{\text{SNR}}$  at the maxima in Fig. 5. All modes are seen to fall in the range  $R_{\text{SNR}} > 33$  dB, where quasi-linear signal transmission along an optical fiber is impossible. In addition, it is interesting that all curves reach their maxima at the ratio  $T_b/T_{FWHM} = 1.7$ , as is seen in Fig. 6a.

As follows from the estimation of the cloud size in a constellation diagram, the theoretically achieved modulation order  $M$ , e.g., at the maximum of the curve for  $T_b = 800$  ps, is 12.9. Thus, at the chosen parameters, error-free data transmission is possible for modulation format 8-PSK (Fig. 6b). Numerical calculations with modulation format 8-PSK for  $T_b = 800$  ps support a high quality of data transmission. Despite the noises in a time indicator diagram, the clouds in a constellation diagram are not overlapped and the frequency channels in the signal spectrum at a detector are well resolved.

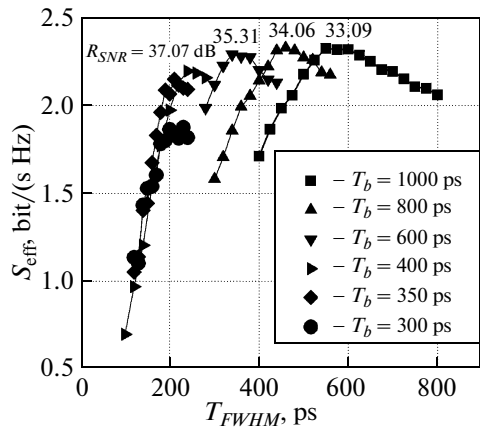


**Fig. 5.** Spectral efficiency vs. soliton signal width  $T_{FWHM}$  for various bit slots  $T_b$ .

For the ratio of the bit slot to the soliton width  $k = 1.7$ , neighboring pulses are significantly overlapped and interact strongly with each other, in contrast to the case of, e.g.,  $k = 5$  (Fig. 7a). Since an information-carrying pulse phase is randomly specified, this leads to interference and nonuniform summation of the signal amplitudes in different time intervals. As a result, pulses have different peak powers and can be shifted from the central position in a bit slot (Fig. 7b). This mode differs substantially from the traditional use of well separated solitons (Fig. 7a). Thus, the initial distribution of soliton pulses at  $k = 1.7$  has nonzero timing and phase jitters.

We now analyze the factors that limit the growth of the spectral efficiency, namely, the effects of random pulse time and phase fluctuations. To this end, we numerically simulated the propagation of a sequence of solitons along FOCL from 250 to 5000 km long.

Figures 8a and 8c show the dependences of  $\sigma_\tau$  and  $\sigma_\phi$  on the propagation length at a receiving device before the application of the method of back propagation, and Figs. 8b and 8d depict these dependences after the application of this method. As is seen from Figs. 8a and 8c, initial nonzero values of  $\sigma_\tau$  and  $\sigma_\phi$  exist at the signal source, which is caused by the overlapping of neighboring soliton pulses. Since the  $T_b/T_{FWHM}$  ratio is fixed, the initial values of the jitters are the same for various bit slots. Moreover, this initial value is a certain threshold below which  $\sigma_\tau$  and  $\sigma_\phi$  cannot be compensated by the method of back propagation.

The timing jitters in Figs. 8a and 8b are normalized by the bit slot. As follows from Fig. 8a, the time divergence of solitons having traveled 2000 km is about 37% of the bit slot for  $T_b = 300$  ps and about 33% for  $T_b = 1000$  ps. Figure 8b presents the results of suppression of the accumulated influence of the effects using the procedure of back propagation. These effects are seen to be fully compensated at distances smaller than 2500 km: the time shift of pulses is returned to a level of 27%. Therefore, the main contribution is only made by the initial overlapping of solitons. Thus, the timing jitter can be fully compensated for  $T_b > 300$  ps and propagation distances smaller than 5000 km and cannot be compensated at  $T_b \leq 300$  ps using the procedure of back propagation.

Figures 8c and 8d illustrate the accumulation and suppression of the phase jitter of a pulse. An increase in the cloud sizes in the constellation diagram indicates a larger difference between soliton phases and an increase in the phase jitter.

As follows from Fig. 8c, a pulse phase changes in high-rate communication lines despite the property of soliton to retain its envelope shape during propagation. This change is caused by many factors, such as incomplete mutual compensation of dispersion and

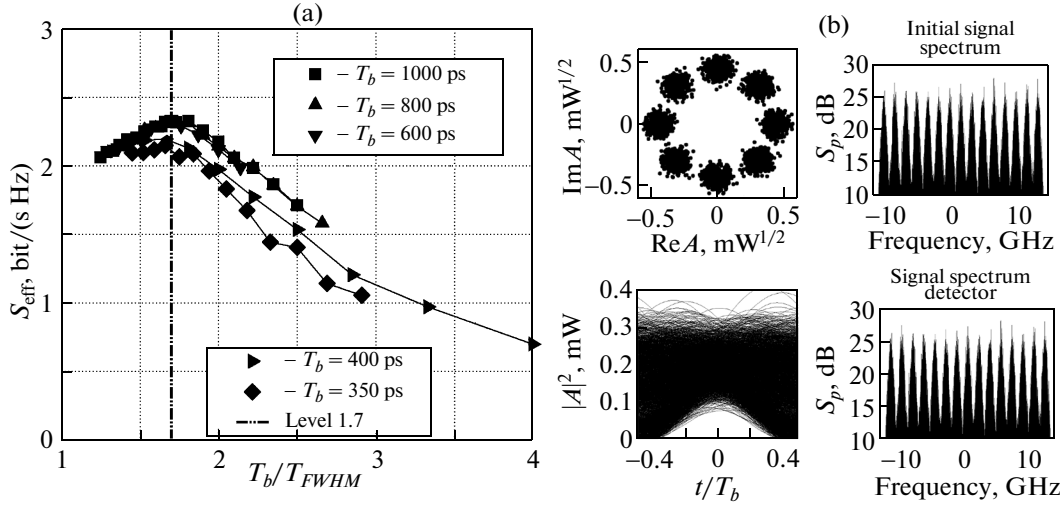


**Fig. 6.** (a) Spectral efficiency vs. ratio  $k = T_b/T_{FWHM}$  and (b) time indicator and constellation diagrams and signal spectra  $S_p$  at the point of maximum  $S_{\text{eff}}$  for  $T_b = 800$  ps.

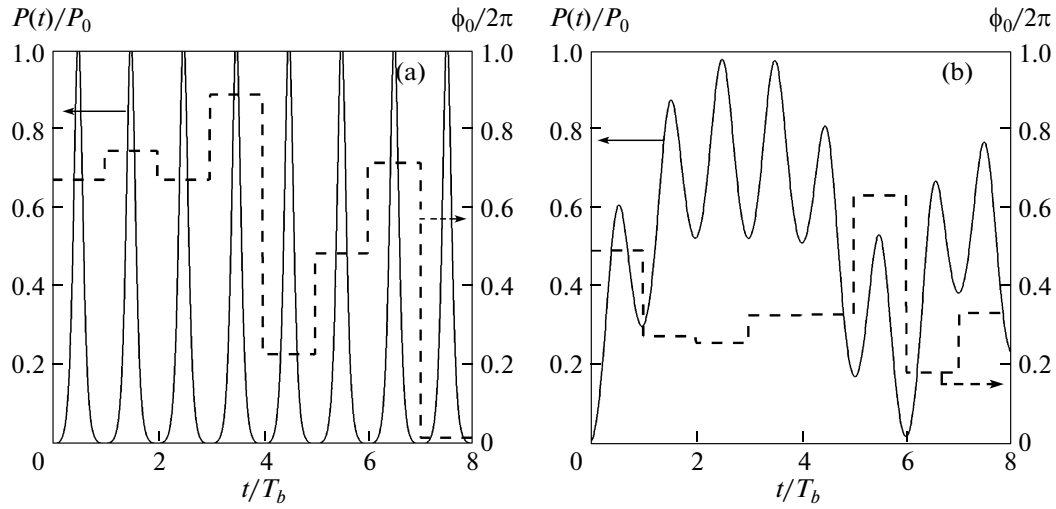


**Fig. 7.** Time envelopes of the field power and the corresponding pulse phases for  $T_b/T_{FWHM} =$  (a) 5 and (b) 1.7.

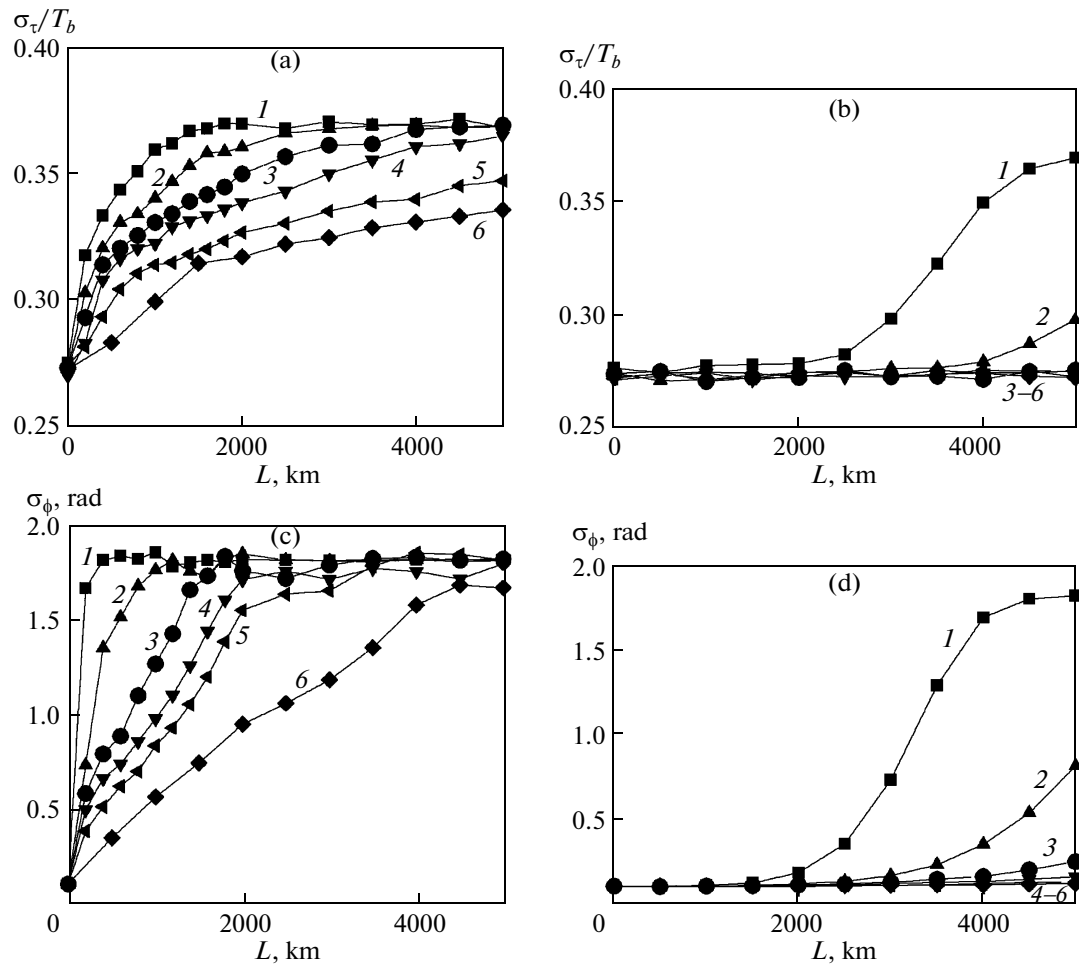


**Fig. 8.** Values of (a) timing and (c) phase jitters before the procedure of back propagation of the signal at a receiving device and (b), (d) after this procedure, respectively, for  $T_b =$  (1) 300, (2) 400, (3) 500, (4) 600, (5) 800, and (6) 1000 ps.

nonlinear distortions, the Gordon–Mollenauer effect, and interchannel interaction. As the phase incursion increases,  $\sigma_\tau$  reaches its limiting value,  $\pi/2$ .

The procedure of back propagation can fully compensate the deterministic (not related to noise) fiber effects and cannot suppress the random irreversible action of nonlinear noise components. For example, the noise of amplifiers is insignificant at small propagation distances. In Fig. 8d, we see the restoration of a signal by the method of back signal propagation at a distance smaller than 1800 km. However, the Gordon–Mollenauer effect remains uncompensated in high-rate communication lines ( $T_b < 300$  ps) at a distance more than 2000 km and is the main limitation of the spectral efficiency growth. As is seen from the curves corresponding to a smaller bit slot, the Gordon–Mollenauer can be compensated at larger distances. The action of nonlinear noise here is weaker as compared to high-rate FOCLs, since the power signal is lower.

## 5. CONCLUSIONS

Thus, we numerically simulated soliton coherent optical fiber communication lines of various lengths that use Raman amplification scheme. It was shown that soliton communication lines can operate at high values of  $R_{SNR}$  and that the maximum spectral efficiency is achieved at a certain ratio of the bit slot to the pulse width. We were the first to study soliton FOCLs in terms of the spectral efficiency.

## ACKNOWLEDGMENTS

This work was supported by the Ministry of Education and Science of the Russian Federation (project no. 14.V25.31.0003), project UNLOC (EPSRC, EP/J017582/1), and the Russian Foundation for Basic Research (project no. 14-01-31258 mol\_a).

## REFERENCES

1. S. P. Novikov, S. V. Manakov, L. P. Pitaevskii, and V. E. Zakharov, *Theory of Solitons: The Inverse Scattering Method* (Consultants Bureau, New York, 1984).
2. A. Hasegawa and Y. Kodama, *Solitons in Optical Communications* (Oxford University Press, Oxford, United Kingdom, 1995).
3. L. F. Mollenauer and J. P. Gordon, *Solitons in Optical Fibers: Fundamentals and Applications* (Academic, San Diego, California, United States, 2006).
4. Yu. S. Kivshar and G. P. Agrawal, *Optical Solitons: From Fibers to Photonic Crystals* (Academic, San Diego, California, United States, 2003).
5. S. K. Turitsyn, B. Bale, and M. P. Fedoruk, Phys. Rep. **521**, 135 (2012).

6. S. K. Turitsyn, E. G. Shapiro, S. B. Medvedev, M. P. Fedoruk, and V. K. Mezentsev, C. R. Phys. **4**, 145 (2003).
7. A. Hasegawa and F. Tappert, Appl. Phys. Lett. **23**, 142 (1973).
8. L. F. Mollenauer, R. H. Stolen, and J. P. Gordon, Phys. Rev. Lett. **45**, 1095 (1980).
9. L. F. Mollenauer and K. Smith, Opt. Lett. **13**, 675 (1988).
10. L. F. Mollenauer, P. V. Mamyshev, and J. P. Gordon, in *Optical Fiber Telecommunications*, Ed. by T. L. Koch (Academic, San Diego, California, United States, 1997), Vol. IIIA, Chap. 10.
11. E. Iannone, F. Matera, A. Mecozzi, and M. Settembre, *Nonlinear Optical Communication Networks* (Wiley, New York, 1998), Chap. 5.
12. E. B. Desurvire, J. Lightwave Technol. **24**, 4697 (2006).
13. D. Hillercus and R. Schmogrow, Nat. Photonics **5**, 364 (2011).
14. E. Ip and J. M. Kahn, J. Lightwave Technol. **26**, 3416 (2008).
15. S. Shieh and I. Djordjevic, *OFDM for Optical Communications* (Academic, New York, 2010).
16. R. Schmogrow, M. Winter, and M. Meyer, Opt. Express **20**, 317 (2011).
17. R.-J. Essiambre and P. J. Winzer, J. Lightwave Technol. **28**, 662 (2010).
18. R.-J. Essiambre, G. J. Foschini, G. Kramer, and P. J. Winzer, Phys. Rev. Lett. **101**, 163901 (2008).
19. A. D. Ellis, J. Zhao, and D. Cotter, J. Lightwave Technol. **28**, 423 (2010).
20. J. D. Ania-Castanon, V. Karalekas, P. Harper, and S. K. Turitsyn, Phys. Rev. Lett. **101**, 123903 (2008).
21. T. J. Ellingham, J. D. Ania-Castanon, R. Ibbotson, X. Chen, L. Zhang, and S. K. Turitsyn, IEEE Photonics Technol. Lett. **18**, 268 (2006).
22. W. Forysiak and N. Doran, J. Lightwave Technol. **13**, 850 (1995).
23. L. F. Mollenauer, J. P. Gordon, and S. G. Evangelides, Opt. Lett. **17**, 1575 (1992).
24. P. V. Mamyshev and L. F. Mollenauer, Opt. Lett. **19**, 2083 (1994).
25. S. L. Jansen and P. M. Krumrich, IEEE Photonics Technol. Lett. **17**, 923 (2005).
26. C. J. McKinstry, S. Radic, and C. Xie, Opt. Lett. **28**, 1519 (2003).
27. J. E. Prilepsky, S. A. Derevyanko, and S. K. Turitsyn, Phys. Rev. Lett. **108**, 183902 (2012).
28. S. Amiralizadeh, A. Nguyen, and L. Rusch, Opt. Express **21**, 20376 (2013).
29. T. Tanimura, M. Nolle, J. K. Fisher, and C. Schubert, in *Theses of the 38th European Conference and Exhibition on Optical Communications (ECOC 2012)*, Amsterdam, The Netherlands, September 16–20, 2012 (Amsterdam, 2012).

*Translated by K. Shakhevich*